

Combining inherent knowledge of vision-language models with unsupervised domain adaptation through strong-weak guidance

Thomas Westfechtel¹, Dexuan Zhang¹, Tatsuya Harada^{1,2}

¹The University of Tokyo ²RIKEN

Tokyo, Japan

{thomas, dexuan.zhang, harada}@mi.t.u-tokyo.ac.jp

Abstract

Unsupervised domain adaptation (UDA) tries to overcome the tedious work of labeling data by leveraging a labeled source dataset and transferring its knowledge to a similar but different target dataset. Meanwhile, current vision-language models exhibit remarkable zero-shot prediction capabilities. In this work, we combine knowledge gained through UDA with the inherent knowledge of vision-language models. We introduce a strong-weak guidance learning scheme that employs zero-shot predictions to help align the source and target dataset. For the strong guidance, we expand the source dataset with the most confident samples of the target dataset. Additionally, we employ a knowledge distillation loss as weak guidance. The strong guidance uses hard labels but is only applied to the most confident predictions from the target dataset. Conversely, the weak guidance is employed to the whole dataset but uses soft labels. The weak guidance is implemented as a knowledge distillation loss with (shifted) zero-shot predictions. We show that our method complements and benefits from prompt adaptation techniques for vision-language models. We conduct experiments and ablation studies on three benchmarks (OfficeHome, VisDA, and DomainNet), outperforming state-of-the-art methods. Our ablation studies further demonstrate the contributions of different components of our algorithm.

1. Introduction

Deep neural networks have significantly advanced the field of computer vision. However, training these networks requires a large amount of labeled data. Unsupervised domain adaptation (UDA) offers a solution by transferring knowledge from a labeled similar but distinct source dataset to an unlabeled target dataset, reducing the need for extensive labeling.

On the other hand, vision-language models exhibit re-

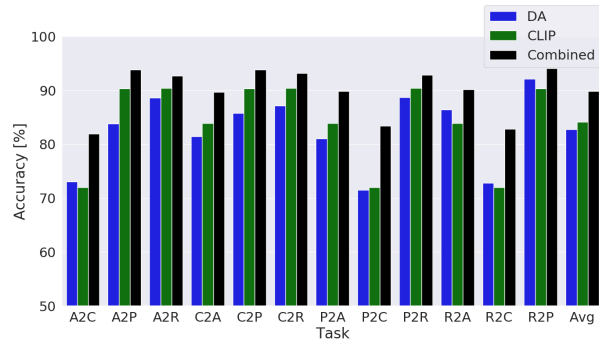


Figure 1. Accuracy on the OfficeHome dataset for unsupervised domain adaptation (blue), CLIP zero-shot predictions (green), and our combined version (black) integrating zero-shot predictions into UDA. In this work, we present a way to combine the knowledge from vision-language models with knowledge transferred via UDA from a source domain. It can be seen that the performance significantly improves.

markable zero-shot prediction accuracy, even without any task-specific training data. For instance, on the DomainNet dataset, current vision-language models’ zero-shot predictions outperform state-of-the-art domain adaptation without the need for a source dataset. This raises the question of the importance of domain adaption method give the rapid emergence of larger foundation models.

In this work, we argue that rather than seeing these two methods as competing, combining the strengths of both of them achieves even better results. We combine the inherent knowledge of the vision-language models with the knowledge transferred from a source dataset through domain adaptation.

To preserve the inherent knowledge of the vision-language model we employ a strong-weak guidance. The strong guidance is applied only for the most confident samples using the hard predictions (i.e. pseudo-label) in form of a source dataset expansion. Conversely, the weak guidance employs soft predictions and is applied to all samples

in form of a knowledge distillation loss. We show that adjusting the temperature parameter of the softmax function enhances the effectiveness of knowledge distillation by accentuating the winning probabilities.

By combining our strong-weak guidance with a conventional unsupervised domain adaptation method we can significantly increase the performance as can be seen in Fig. 1. This highlights the potential of combining inherent knowledge of vision-language models with knowledge transferred from a source domain.

While much research on domain adaptation with CLIP models has focused on adapting the text prompt, our method focuses on adapting the visual encoder, while maintaining its inherent knowledge. We show that these two approaches are complementary, and show that our method benefits from combining it with the prompt adaptation method DAPL [7].

Our main contributions are:

- We introduce a strong-weak guidance scheme to exploit inherent knowledge of vision-language models and combine it with a conventional UDA method.
- We introduce a combination of weak guidance based on knowledge distillation of shifted zero-shot predictions and strong guidance based on source dataset expansion.
- We show the effectiveness of our algorithm on three datasets (Office-Home, VisDA, and DomainNet) and further evaluate the method in various ablation studies.
- We show that the method is applicable for both CNN-based and ViT-based backbones.

2. Related works

2.1. Unsupervised domain adaptation

The goal of unsupervised domain adaptation is to overcome the domain shift between the source and the target dataset. Surveys for this task can be found in [39], [36]. One approach is to align the feature space distributions between the two datasets. Domain-adversarial neural network (DANN) [5] introduces an adversarial approach to achieve this. A domain classifier is trained to distinguish the feature space of source and target samples. The work introduced a gradient reversal layer. This layer inverts the gradients and thereby inverts the training objective, meaning that the backbone is trained to generate features that are indistinguishable for the domain classifier, generating so-called domain invariant features. BIWAA introduces a feature reweighting approach based on their contribution to the classifier. CDAN [16] extended DANN by multilinear conditioning the domain classifier with the classifier predictions. Moving semantic transfer network [31] introduced a moving semantic loss.

Another approach employs information maximization or entropy minimization to generate more accurate target predictions. SHOT [15] exploits both information maximization and self-supervised pseudo-labeling to increase the performance of the target domain. SENTRY [22] uses prediction consistency among different augmentations of an image to either minimize its entropy or maximize it in case of inconsistent predictions.

Following the rise of vision transformers approaches specially tailored for these backbones have gained popularity. TVT [33] introduced a Transferability Adaption Module that employs a patch-level domain discriminator to measure the transferability of patch tokens, and injects learned transferability into the multi-head self-attention block of a transformer. CDTrans [32] introduced a triple-branch transformer framework with cross-attention between source and target domains. PMTrans [38] introduced PatchMix which builds an intermediate domain by mixing patches of source and target images. The mixing process uses a learnable Beta distribution and attention-based scoring function to assign label weights to each patch.

In our work, we employ CDAN [16] as our domain adaptation loss. While the performance is neither state-of-the-art for CNN-based nor transformer-based networks, it achieves reasonable performance for both architectures. [11] has shown that many algorithms developed for CNN backbones underperform for transformer-based backbones. On the other hand, most transformer-based algorithms explicitly make use of the network structure and cannot be employed for CNN-backbones.

2.2. Vision-language models

CLIP [23] introduced a contrastive learning strategy between text and image pairs. It employs a text encoder and a visual encoder. Feature representations of positive pairs are pushed together, while unrelated or negative pairs are pushed apart. The usage of visual and language encoders enables zero-shot prediction. The class labels are encoded via the language encoder and serve as classifier. Usually, the class labels are combined with a pretext or ensemble of pretexts such as 'A photo of a {object}.' to enhance the performance, where {object} is replaced with the respective classes. While CLIP collected the training dataset by constructing an allowlist of high-frequency visual concepts from Wikipedia, ALIGN [9] does not employ this step, but makes up for it by using a much larger, though noisier, dataset. BASIC [21] further increased the zero-shot prediction capabilities by further increasing data size, model size, and batch size. LiT [35] employs a pre-trained image encoder as visual backbone and aligns a text encoder to it. The vision encoder is frozen during the alignment. DFN [4] investigates data filtering networks to pool high-quality data from noisy curated web data.

In our work, we employ the CLIP pre-trained models due to their popularity. We employ the seven ImageNet templates subset published on the CLIP Git Hub.

2.3. Domain adaptation for vision-language models

Surprisingly there has not been much research on combining domain adaptation to vision-language models.

Few approaches make use of prompt learning [37]. This approach trains the prompt’s context words for the text encoder with learnable vectors while the encoder weights are frozen. DAPL [7] employs a prompt learning approach to learn domain-agnostic context variables and domain-specific context variables for unsupervised domain adaptation. This approach freezes the text and vision encoder during training. AD-CLIP [25] introduces a prompt learning scheme that entirely leverages the visual encoder of CLIP and introduces a small set of learnable projector networks. PADCLIP [12] aims for a debiasing zero-shot predictions and employs a self-training paradigm, we employ adjusted prediction scores instead of hard pseudo-labels and use an adversarial approach to overcome the domain gap. EUDA [13] employs prompt task-dependant tuning and a visual feature refinement module in combination with pseudo-labeling from semi-supervised classifiers. MPA [2] takes a similar approach of prompt learning for multi-source unsupervised domain adaptation. In a first step, individual prompts are learned to minimize the domain gap through a contrastive loss. Then, MPA employs an auto-encoding process and aligns the learned prompts by maximizing the agreement of all the reconstructed prompts. DALL-V [34] employs large language-vision models for the task of source-free video domain adaptation. They distill the world prior and complementary source model information into a student network tailored for the target. This approach also freezes the vision encoder and only learns an adapter on top of the vision encoder.

Unlike most of the above methods, we do not freeze the vision encoder during the training. While most of the mentioned methods focus on adapting the text prompts, we focus on adapting the visual extractor while retaining the inherent knowledge through knowledge distillation. We also show our method is complementary to and benefits from prompt learning methods.

3. Methodology

In unsupervised domain adaptation, the goal is to transfer knowledge from a source dataset \mathcal{D}_s consisting of n_s labeled images $\mathcal{D}_s = (x_{i,s}, y_{i,s})_{i=1}^{n_s}$ to an unlabeled target dataset \mathcal{D}_t containing n_t unlabeled data $\mathcal{D}_t = (x_{i,t})_{i=1}^{n_t}$. In this work we focus on combining the inherent knowledge of vision-language models with the knowledge gained from the knowledge transfer of the source domain, meaning we

further have access to the zero-shot predictions y_o for each sample.

For the knowledge transfer from the source to the target domain, we employ the widely established adversarial domain adaptation method CDAN [16] as it was shown to be effective for both convolutional- and transformer-based network architectures [11].

To preserve the inherent knowledge of the vision-language model we employ a strong-weak guidance scheme. For the strong guidance, a hard pseudo-label is employed, but only for the most confident samples. We employ a source domain expansion inspired by GSDE [30] that copies the most confident target samples into the source domain with their predicted pseudo-label.

For the weak guidance, we employ a knowledge distillation loss [8] using the zero-shot predictions. However, since the zero-shot predictions exhibit a relatively wide spread of probabilities among the classes (see Fig. ??), we first adjust the distribution to accentuate the winning probabilities. The process flow of our algorithm can be seen in Fig. 2.

We use the three losses:

$$L = L_{CE} + L_{KD} + L_{AD} \quad (1)$$

where L_{CE} is the classification loss for the source data, L_{KD} is the knowledge distillation loss, and L_{AD} is the adversarial adaptation loss. L_{KD} and L_{AD} are calculated for both source and target data. We further employ a strongly augmented version of source and target data, which are handled in the same way as the weakly augmented versions.

We also show that our method is complementary to prompt learning methods by combining it with Domain Adaptation via Prompt Learning (DAPL) [7].

3.1. Strong guidance - Source Domain Expansion:

For the strong guidance, we employ a source domain expansion strategy. The highest scoring zero-shot predictions are copied and appended to the source dataset with their respective pseudo-labels as pseudo-source data. We employ this source domain expansion strategy since it was shown to be more effective than simply adding a CE-loss for the respective target samples (as was shown in [30]). During training no distinction between source data and pseudo-source data is made.

The paper that inspired the strategy for our strong guidance employed the source domain expansion in an iterative procedure. The network was trained for several runs, each time with an increasing amount of pseudo-source data.

In this work, we experiment with 2 different versions. The first version trains the network a single time. The second version employs an iterative training scheme training for 2 runs. In the first run, the source domain expansion is done regarding the zero-shot predictions, and in the second

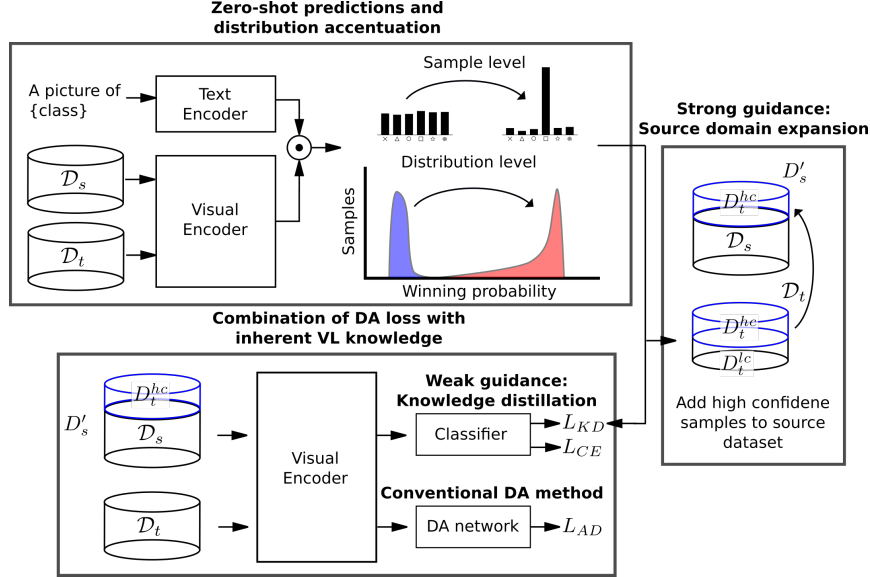


Figure 2. Process flow of our algorithm. In a first step, the zero-shot predictions of source \mathcal{D}_s and target \mathcal{D}_t dataset are estimated. We shift the zero-shot predictions distribution through a temperature parameter in the softmax to accentuate the winning probability. Based on the zero-shot predictions, we extend the source dataset with high confident target samples. These samples are treated as source data, with their respective pseudo-labels and represent the strong guidance of our method. The network is then trained using a classification loss L_{CE} for the (expanded) source data, a knowledge distillation loss L_{KD} employing the shifted zero-shot predictions \tilde{y}_o , and an adversarial adaptation loss L_{DA} . The knowledge distillation loss represents the weak guidance of the method, as it is employed for all samples and uses the soft zero-shot predictions.

run it is done regarding a mixture of zero-shot predictions and predictions generated from the previous run:

$$s(\hat{y}) = p(y_{n-1}) + \frac{1}{2}p(\tilde{y}_o) \quad (2)$$

where $s(\hat{y})$ depicts the scores of the samples for being chosen as pseudo-source samples, $p(y_{n-1})$ depicts the predictions of the previous run, and $p(\tilde{y}_o)$ depicts the zero-shot predictions.

While the first version trains for a single run, and therefore no additional computational time is required, the second version trains for two runs, which require double the training time.

3.2. Weak guidance - Knowledge distillation loss

For the weak guidance, we employ a knowledge distillation loss [8] using the zero-shot predictions. However, since the predictions are rather evenly spread among all classes, we shift the distribution before employing them in the KD-loss (see Fig. 2). This is done through a temperature parameter T in the softmax function. In a normal KD setting, the teacher’s winning prediction score usually tends to approach a one-hot vector. The goal is to mimic this distribution while maintaining the relative prediction probabilities. To accomplish that we estimate the temperature parameter T so that the mean winning probability equals to τ . We

employ a value of $\tau = 0.9$ in our experiments. In the estimation, we equally factor the source and target domain to further maintain the relative prediction confidence between the two domains.

$$\frac{1}{2n_s} \sum_{n_s} \max(\sigma(y_{o,i,s}/T)) + \frac{1}{2n_t} \sum_{n_t} \max(\sigma(y_{o,i,t}/T)) = \tau \quad (3)$$

$y_{o,i,s}$ depicts logits of the i -th sample of the source data the σ depicts the softmax-function. We then employ the shifted zero-shot predictions for the knowledge distillation loss:

$$L_{KD} = D_{KL}(\tilde{y}_o || y) \quad (4)$$

where D_{KL} is the Kullback-Leibler divergence loss, and y is the output of the classifier of our network.

3.3. Adversarial loss

We employ conditional adversarial domain adaptation loss CDAN:

$$L_{AD} = L_{BCE}(G_d((f_i \otimes p_i), d_i)) \quad (5)$$

where G_d is the domain classification network. f_i are the features of sample i , p_i the class probabilities and d_i the domain label. CDAN employs a gradient reversal layer to

Table 1. Accuracy results on Office-Home dataset. The best results are displayed in bold and the runner-up results are underlined. Methods using a ResNet-50 backbone are on top, and methods using a transformer-based backbone are on the bottom. CLIP indicates zero-shot results of CLIP, and methods based on it are listed below it. Our methods are on the bottom, DAPL marks the combination with the prompt learning method. V1 stands for version 1 and V2 for version 2 respectively.

Method - RN50	A→C	A→P	A→R	C→A	C→P	C→R	P→A	P→C	P→R	R→A	R→C	R→P	Avg
CDAN [16]	50.7	70.6	76.0	57.6	70.0	70.0	57.4	50.9	77.3	70.9	56.7	81.6	65.8
SRDC [27]	52.3	76.3	81.0	69.5	76.2	78.0	68.7	53.8	81.7	76.3	57.1	85.0	71.3
BIWAA-I [29]	56.3	78.4	81.2	68.0	74.5	75.7	67.9	56.1	81.2	75.2	60.1	83.8	71.5
Sentry [22]	61.8	77.4	80.1	66.3	71.6	74.7	66.8	63.0	80.9	74.0	66.3	84.1	72.2
GSDE [30]	57.8	80.2	81.9	71.3	78.9	80.5	67.4	57.2	84.0	76.1	62.5	85.7	73.6
PCL [14]	60.8	79.8	81.6	70.1	78.9	78.9	69.9	60.7	83.3	77.1	66.4	85.9	74.5
CLIP [23]	48.5	81.2	83.5	72.6	81.2	83.5	72.6	48.5	83.5	72.6	48.5	81.2	71.5
DAPL [7]	54.1	84.3	84.8	74.4	83.7	85.0	74.5	54.6	84.8	75.2	54.7	83.8	74.5
AD-CLIP [25]	55.4	85.2	85.6	76.1	85.8	86.2	76.7	56.1	85.4	76.8	56.1	85.5	75.9
PADCLIP [12]	57.5	84.0	83.8	77.8	85.5	84.7	76.3	59.2	85.4	78.1	60.2	86.7	76.6
EUDA [13]	58.1	85.0	84.5	77.4	85.0	84.7	76.5	58.8	85.7	75.9	60.4	86.4	76.5
SWG V1	64.5	85.9	86.8	78.6	87.8	86.7	79.5	64.9	86.7	80.6	66.0	88.9	79.7
SWG V2	66.1	87.5	86.7	79.5	87.3	86.4	79.4	66.9	87.1	80.3	68.1	88.7	80.4
SWG DAPL V1	<u>70.8</u>	88.9	<u>89.1</u>	<u>80.5</u>	90.3	<u>88.7</u>	<u>81.2</u>	<u>71.3</u>	<u>89.1</u>	<u>83.8</u>	<u>74.4</u>	<u>92.0</u>	<u>83.3</u>
SWG DAPL V2	74.4	<u>88.5</u>	89.6	81.1	<u>89.3</u>	89.3	82.4	74.3	89.4	84.2	76.8	92.1	84.3
Method - ViT	A→C	A→P	A→R	C→A	C→P	C→R	P→A	P→C	P→R	R→A	R→C	R→P	Avg
CDAN [16]	62.6	82.9	87.2	79.2	84.9	87.1	77.9	63.3	88.7	83.1	63.5	90.8	79.3
TVT [33]	74.9	86.8	89.5	82.8	88.0	88.3	79.8	71.9	90.1	85.5	74.6	90.6	83.6
CDTrans [32]	68.8	85.0	86.9	81.5	87.1	87.3	79.6	63.3	88.2	82.0	66.0	90.6	80.5
SDAT [24]	70.8	87.0	90.5	85.2	87.3	89.7	84.1	70.7	90.6	88.3	75.5	92.1	84.3
SSRT [26]	75.2	89.0	91.1	85.1	88.3	89.9	85.0	74.2	91.2	85.7	78.6	91.8	85.4
PMTrans [38]	81.3	92.9	92.8	88.4	93.4	93.2	87.9	80.4	93.0	89.0	80.9	94.8	89.0
CLIP [23]	66.8	89.1	89.7	83.3	89.1	89.7	83.3	66.8	89.7	83.3	66.8	89.1	82.2
DAPL [7]	70.6	90.2	91.0	84.9	89.2	90.9	84.8	70.5	90.6	84.8	70.1	90.8	84.0
AD-CLIP [25]	70.9	92.5	92.1	85.4	92.4	92.5	86.7	74.3	93.0	86.9	72.6	93.8	86.1
PADCLIP [12]	76.4	90.6	90.8	86.7	92.3	92.0	86.0	74.5	91.5	86.9	79.1	93.1	86.7
EUDA [13]	78.2	90.4	91.0	87.5	91.9	92.3	86.7	79.7	90.9	86.4	79.4	93.5	87.3
SWG V1	81.7	93.2	93.0	89.2	93.4	92.7	89.6	82.8	92.7	90.2	83.4	94.1	89.7
SWG V2	81.9	<u>93.9</u>	92.7	<u>89.7</u>	93.8	93.2	89.8	83.4	92.8	90.2	82.8	94.1	89.9
SWG DAPL V1	<u>85.2</u>	94.0	<u>93.2</u>	89.5	<u>94.2</u>	<u>93.8</u>	<u>90.5</u>	<u>87.0</u>	<u>94.0</u>	<u>91.9</u>	<u>87.2</u>	<u>95.2</u>	<u>91.3</u>
SWG DAPL V2	87.7	<u>93.9</u>	94.1	91.3	94.3	94.0	91.6	89.0	94.1	92.5	89.4	95.7	92.3

inverse the training objective. This means that while the domain classifier is trained to distinguish the domain (source or target) of the respective sample, the objective of the feature extractor is to extract features that are indistinguishable for the domain classifier, thereby generating domain invariant features.

3.4. Further improvements:

3.4.1 Batch norm layer adjustment

The ResNet backbone employs batch norm layers. However, the distribution of the pretraining data is vastly dif-

ferent than the data used for the domain adaptation. The running average and mean change abruptly at the beginning of the adaptation process, shifting the data out of the learned distribution and resulting in failure. One solution would be to freeze the batch norm layers, but this can result in exploding feature norms, making the training unstable. In our work, we estimate the average and mean for the source and target data for each batch norm layer and adjust the learnable parameters β and γ so that the running mean and var equals that of our training data.

Table 2. Accuracy results on VisDA dataset. The best results are displayed in bold and the runner-up results are underlined. Methods using a ResNet-101 backbone are on top, and methods using a transformer-based backbone are on the bottom. CLIP indicates zero-shot results of CLIP, and methods based on it are listed below it. Our methods are on the bottom, DAPL marks the combination with the prompt learning method. V1 stands for version 1 and V2 for version 2 respectively.

Method - RN101	plane	bcycl	bus	car	horse	knife	mcycl	person	plant	sktbrd	train	truck	Avg
CDAN [16]	85.2	66.9	83.0	50.8	84.2	74.9	88.1	74.5	83.4	76.0	81.9	38.0	73.9
CGDM [3]	93.4	82.7	73.2	68.4	92.9	94.5	88.7	82.1	93.4	82.5	86.8	49.2	82.3
STAR [17]	95.0	84.0	84.6	73.0	91.6	91.8	85.9	78.4	94.4	84.7	87.0	42.2	82.7
CAN [10]	97.0	87.2	82.5	74.3	97.8	<u>96.2</u>	90.8	80.7	96.6	96.3	87.5	59.9	87.2
CoVi [18]	96.8	85.6	88.9	88.6	97.8	93.4	91.9	87.6	<u>96.0</u>	93.8	93.6	48.1	88.5
CLIP [23]	98.0	83.3	90.8	65.9	97.8	83.0	93.4	67.7	85.2	90.0	94.9	66.4	84.7
DAPL [7]	97.8	83.1	88.8	77.9	97.4	91.5	94.2	79.7	88.6	89.3	92.5	62.0	86.9
AD-CLIP [25]	98.1	83.6	91.2	76.6	98.1	93.4	96.0	81.4	86.4	91.5	92.1	64.2	87.7
PADCLIP [12]	96.7	88.8	87.0	82.8	97.1	93.0	91.3	83.0	95.5	91.8	91.5	63.0	88.5
EUDA [13]	97.2	<u>89.3</u>	87.6	<u>83.1</u>	98.4	95.4	92.2	82.5	94.9	93.2	91.3	64.7	89.2
SWG V1	99.0	86.3	92.4	73.7	98.9	97.1	95.6	82.2	91.4	96.0	93.7	<u>73.1</u>	90.0
SWG V2	<u>98.9</u>	87.5	90.9	74.5	<u>98.6</u>	95.9	95.8	<u>83.5</u>	90.5	96.3	<u>93.8</u>	76.6	90.2
SWG DAPL V1	99.0	86.9	92.4	80.0	98.3	94.5	<u>95.9</u>	82.5	92.7	<u>96.6</u>	92.8	69.4	<u>90.1</u>
SWG DAPL V2	98.7	89.7	<u>92.3</u>	82.6	98.4	93.8	95.3	82.1	91.8	97.5	93.5	66.7	90.2
Method - ViT	plane	bcycl	bus	car	horse	knife	mcycl	person	plant	sktbrd	train	truck	Avg
SHOT [15]	99.5	91.8	88.7	65.1	98.6	98.0	96.0	66.1	95.1	98.9	<u>96.8</u>	52.4	87.3
PMTrans [38]	99.4	88.3	88.1	78.9	98.8	<u>98.3</u>	95.8	70.3	94.6	98.3	96.3	48.5	88.0
SSRT [26]	98.9	87.6	89.1	84.8	98.3	98.7	96.3	81.1	94.8	97.9	94.5	43.1	88.8
AdaCon [1]	99.5	94.2	91.2	83.7	98.9	97.7	96.8	71.5	<u>96.0</u>	98.7	97.9	45.0	89.2
DePT-D [6]	99.4	93.8	<u>94.4</u>	87.5	99.4	98.0	<u>96.7</u>	74.3	98.4	98.5	96.6	51.0	90.7
CLIP [23]	99.3	91.5	92.9	71.0	99.4	92.7	94.4	75.6	84.7	97.4	95.5	69.0	88.6
DAPL [7]	99.2	92.5	93.3	75.4	98.6	92.8	95.2	82.5	89.3	96.5	95.1	63.5	89.5
AD-CLIP [25]	99.6	92.8	94.0	78.6	98.8	95.4	96.8	83.9	91.5	95.8	95.5	65.7	90.7
PADCLIP [12]	98.1	93.8	87.1	<u>85.5</u>	98.0	96.0	94.4	86.0	94.9	93.3	93.5	70.2	90.9
EUDA [13]	98.4	94.3	89.0	85.4	98.5	<u>98.3</u>	96.1	<u>86.3</u>	95.1	95.2	92.5	<u>70.9</u>	91.7
SWG V1	99.8	94.2	94.3	74.8	<u>99.6</u>	98.7	96.8	81.4	90.9	99.1	96.9	67.8	91.2
SWG V2	<u>99.7</u>	<u>95.6</u>	93.0	74.1	99.7	<u>98.3</u>	96.6	82.9	91.5	99.3	96.9	71.1	91.6
SWG DAPL V1	99.6	94.8	94.5	79.0	99.2	<u>98.3</u>	96.8	86.2	92.8	<u>99.2</u>	96.0	67.2	<u>92.0</u>
SWG DAPL V2	99.5	96.8	93.5	83.2	99.4	98.7	95.5	86.8	93.5	99.1	96.2	70.0	92.7

$$\tilde{\beta} = \beta - (\mu_p - \mu_c) * \frac{\gamma}{\sqrt{\sigma_p}} \quad (6)$$

$$\tilde{\gamma} = (\gamma * \frac{\sqrt{\sigma_c}}{\sqrt{\sigma_p}}) \quad (7)$$

where μ_p and σ_p represent the running mean and variance of the pre-trained model, and μ_c and σ_c represent the estimated mean and variance of the training data.

3.4.2 Zero-shot predictions

To increase the quality of zero-shot predictions, we try to keep the original ratios of the images. The smaller side of an image gets resized to 224 pixels and the larger side gets

resized by the same factor but rounded to the closes multiple of 16 - according to the patchsize of the ViT-backbone (32 for ResNet-backbone due to the attention pooling). We interpolate the positional embedding in order for the network to process the different image sizes.

3.4.3 DAPL

Domain Adaptation via Prompt Learning (DAPL) [7] focuses on adapting the prompts of the text encoder. It freezes both text and visual encoder during the training. In contrast to this, our method focuses on adapting the visual encoder. The text encoder is only used for the inference of the zero-shot predictions. In this work, we show that these two adaptation strategies are complementary and can easily be com-

Table 3. Accuracy results on DomainNet dataset.

MCD	clp	inf	pnt	qdr	rel	skt	Avg	SCDA	clp	inf	pnt	qdr	rel	skt	Avg	CDTrans	clp	inf	pnt	qdr	rel	skt	Avg
clp	-	15.4	25.5	3.3	44.6	31.2	24.0	clp	-	18.6	39.3	5.1	55.0	44.1	32.4	clp	-	29.4	57.2	26.0	72.6	58.1	48.7
inf	24.1	-	24.0	1.6	35.2	19.7	20.9	inf	29.6	-	34.0	1.4	46.3	25.4	27.3	inf	57.0	-	54.4	12.8	69.5	48.4	48.4
pnt	31.1	14.8	-	1.7	48.1	22.8	23.7	pnt	44.1	19.0	-	2.6	56.2	42.0	32.8	pnt	62.9	27.4	-	15.8	72.1	53.9	46.4
qdr	8.5	2.1	4.6	-	7.9	7.1	6.0	qdr	30.0	4.9	15.0	-	25.4	19.8	19.0	qdr	44.6	8.9	29.0	-	42.6	28.5	30.7
rel	39.4	17.8	41.2	1.5	-	25.2	25.0	rel	54.0	22.5	51.9	2.3	-	42.5	34.6	rel	66.2	31.0	61.5	16.2	-	52.9	45.6
skt	37.3	12.6	27.2	4.1	34.5	-	23.1	skt	55.6	18.5	44.7	6.4	53.2	-	35.7	skt	69.0	29.6	59.0	27.2	72.5	-	51.5
Avg	28.1	12.5	24.5	2.4	34.1	21.2	20.5	Avg	42.6	16.7	37.0	3.6	47.2	34.8	30.3	Avg	59.9	25.3	52.2	19.6	65.9	48.4	45.2
SSRT	clp	inf	pnt	qdr	rel	skt	Avg	PMTrans	clp	inf	pnt	qdr	rel	skt	Avg	EUDA	clp	inf	pnt	qdr	rel	skt	Avg
clp	-	33.8	60.2	19.4	75.8	59.8	49.8	clp	-	34.2	62.7	32.5	79.3	63.7	54.5	clp	-	54.8	69.9	35.3	85.1	67.4	62.5
inf	55.5	-	54.0	9.0	68.2	44.7	46.3	inf	67.4	-	61.1	22.2	78.0	57.6	57.3	inf	70.2	-	68.5	16.6	82.2	65.9	60.7
pnt	61.7	28.5	-	8.4	71.4	55.2	45.0	pnt	69.7	33.5	-	23.9	79.8	61.2	53.6	pnt	72.4	54.6	-	29.5	83.0	66.4	61.2
qdr	42.5	8.8	24.2	-	37.6	33.6	29.3	qdr	54.6	17.4	38.9	-	49.5	41.0	40.3	qdr	73.1	50.8	64.3	-	81.2	62.3	66.3
rel	69.9	37.1	66.0	10.1	-	58.9	48.4	rel	74.1	35.3	70.0	25.4	-	61.1	53.2	rel	75.5	56.1	74.6	30.2	-	65.6	60.4
skt	70.6	32.8	62.2	21.7	73.2	-	52.1	skt	73.8	33.0	62.6	30.9	77.5	-	55.6	skt	74.9	56.2	70.2	32.3	80.3	-	62.8
Avg	60.0	28.2	53.3	13.7	65.3	50.4	45.2	Avg	67.9	30.7	59.1	27.0	72.8	56.9	52.4	Avg	73.2	54.5	69.5	28.8	82.4	65.5	62.3
PADCLIP	clp	inf	pnt	qdr	rel	skt	Avg	SWG V1	clp	inf	pnt	qdr	rel	skt	Avg	SWG V2	clp	inf	pnt	qdr	rel	skt	Avg
clp	-	55.1	71.1	36.8	84.2	68.1	63.1	clp	-	58.4	73.1	25.7	85.0	71.9	62.8	clp	-	58.2	74.0	30.4	85.4	72.7	64.2
inf	73.6	-	70.6	18.0	83.5	66.6	62.5	inf	78.7	-	73.1	24.7	84.8	70.8	66.4	inf	79.7	-	73.7	28.5	85.3	71.2	67.7
pnt	75.4	54.3	-	32.0	83.5	67.2	62.5	pnt	79.6	58.3	-	26.0	84.6	71.3	63.9	pnt	80.3	58.4	-	27.8	84.8	71.9	64.6
qdr	74.6	53.6	70.0	-	83.1	66.1	69.5	qdr	76.5	56.2	70.6	-	84.0	69.2	71.3	qdr	76.3	53.5	71.4	-	83.8	69.6	70.9
rel	76.4	54.9	72.7	31.7	-	67.5	60.6	rel	80.4	58.5	73.9	24.4	-	71.4	61.7	rel	81.2	58.8	74.4	29.6	-	72.0	63.2
skt	76.3	54.9	71.7	34.9	83.6	-	64.3	skt	80.6	58.1	73.6	25.1	84.8	-	64.5	skt	81.6	58.7	74.8	30.5	85.3	-	66.2
Avg	75.3	54.6	71.2	30.7	83.6	67.1	63.7	Avg	79.2	57.9	72.9	25.2	84.6	70.9	65.1	Avg	79.8	57.5	73.7	29.4	84.9	71.5	66.1

bined with each other. In particular, we combine these two methods in a sequential manner. In a first step, we run the DAPL algorithm and use the adapted text prompts to estimate the probabilities for the source and target data, which are then employed instead of the zero-shot predictions.

4. Experiments

We evaluate our proposed method on three different domain adaptation benchmarks, Office-Home, VisDA, and DomainNet. We show that we can improve the baselines significantly. In ablation studies, we further investigate the contribution of the different parts of our proposed algorithm.

4.1. Setup

Office-Home [28] contains 15,500 images of 65 categories. The domains are Art (A), Clipart (C), Product (P), and Real-World (R). We evaluate all twelve possible adaptation tasks.

VisDA [20] is a challenging dataset for synthetic-to-real domain adaptation. The synthetic source domain consists of 152397 images and the real-world target domain consists of 55388 images over 12 different classes.

DomainNet [19] is a large-scale dataset with about 600,000 images from 6 different domains and 345 different classes. We evaluate all 30 possible adaptation tasks.

Implementation details: We built up our implementation on the CDAN implementation of [16]. We do all experiments with the CLIP-trained versions of the ResNet backbone and transformer backbone. For the ResNet backbone, we follow most other publications and employ ResNet-50 for OfficeHome and ResNet-101 for VisDA. For the trans-

former backbone, we employ ViT-B/16. We employ the seven ImageNet templates subset published on the CLIP Git Hub page as text prompts for estimating the zero-shot predictions. For OfficeHome we train each run for 100 episodes, for VisDA and DomainNet we train for 50 episodes. For OfficeHome and DomainNet, we employ AdamW optimizer with a learning rate of $5e^{-6}$ for the backbone and $5e^{-5}$ for the newly initialized layers. For VisDA we employ a lower learning rate of $1e^{-6}$, and $1e^{-5}$ respectively. We employ a batch size of 64. For load each image once with weak and once with strong data augmentation, but don't discriminate between the augmentations in the processing pipeline. We run two different versions of our method. The first version trains with a source expansion set to 50%. The second version trains at first with a source expansion set to 33.3% in a first run, and 66.6% in a second run, where the first run employs the zero-shot predictions and the second a mixture between zero-shot and previous run predictions for the source expansion. Due to the two training runs, the second version requires about double the training time. We employ the official implementation of DAPL for the respective experiments.

4.2. Results

Results for Office-Home: The results for the Office-Home dataset are shown in Tab. 1. All versions of our method vastly outperform earlier work. The addition of DAPL improves the results by around 3 – 4%pts in the case of the ResNet backbone and around 2%pts for the ViT backbone. The second version using an iterative training scheme with 2 runs increases the accuracy in all cases, this comes however at the cost of roughly double the training time.

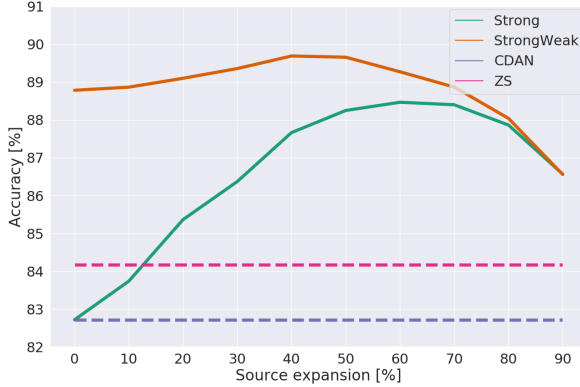


Figure 3. Accuracy for adaptation of OfficeHome dataset for different source domain expansion percentages. The green line employs only the strong guidance, while the orange line employs both guidance. Additionally, the baselines of only using the adversarial domain adaptation (CDAN) and the CLIP zero-shot accuracy (ZS) are plotted.

Results for VisDA-2017: The results for the VisDA-2017 dataset are shown in Tab. 2. Again, our method just by itself already outperforms most of the earlier works. Our method slightly performs worse than EUDA only for the case of the ViT-backbone and without using DAPL. However, once we add DAPL, we outperform the next best-performing method by 1%pts for the ResNet and ViT backbone.

Results for DomainNet: The results for the DomainNet dataset are shown in Tab. 3. The CLIP-based adaptation methods clearly outperform conventional methods by upwards of 10%pts. Our method significantly outperforms current state-of-the-art methods, increasing the average accuracy by 1.4%pts or 2.4%pts respectively over the next best performing method. Version 2, the iterative version of our method increases the accuracy by 1%pts over version 1. This however comes again at the price of the increase in training time.

5. Ablation studies

Combination of strong and weak guidance In this part, we evaluate the effect of combining the strong and weak guidance, as well as the parameter for the percentage of target data that get added to the source dataset. The results can be seen in Fig. 3. It should be noted in the case of 0% source expansion, the strong guidance is equivalent to CDAN, and the strong-weak guidance is equivalent to only weak guidance. The guidance vastly improves over the baselines, and the combination of both even further improves the results. According to the results we chose a source expansion of 50% in the single run experiments of our evaluations.

Parameter for shifting the zero-shot distribution τ : In this part, we evaluate the effect of the parameter τ . Fig. 4

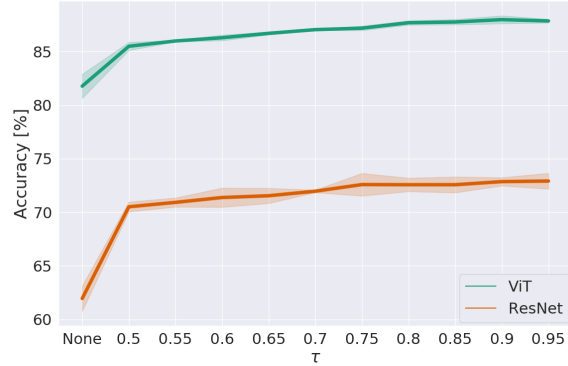


Figure 4. Accuracy for adaptation of OfficeHome C→A for different values for τ . None represents directly using the zero-shot predictions without any distribution shift. It can be seen that adjusting the probability distribution is fundamental for the knowledge distillation to work properly.

shows the accuracy for different values of τ . None means that no distribution shift was applied to the zero-shot predictions. It can be seen that applying the distribution shift is essential for the method. Employing a shift of $\tau = 0.9$ increases the accuracy by 10.9pp for ResNet and 6.2pp for ViT backbone. For the ViT backbone, the accuracy increases constantly until a value of 0.9, for which the accuracy peaks. For the ResNet backbone, it seems that even higher values of τ yield better results. In all our experiments, we employ a value for τ of 0.9.

6. Conclusion

In this work, we presented a novel way to combine the knowledge of vision-language models with knowledge gained from a source dataset through a strong-weak guidance scheme. For the strong guidance, we expand the source dataset with the most confident samples of the target dataset. Additionally, we employ a knowledge distillation loss as weak guidance. The strong guidance uses hard labels but is only applied to the most confident predictions from the target dataset. Conversely, the weak guidance is employed to the whole dataset but uses soft labels. For the domain adaptation loss, we employed CDAN as it is effective for both CNN and ViT-based backbones. Furthermore, we showed that our method is complementary to prompt learning methods and a combination can further improve the accuracy. We showed the effectiveness of our method for both CNN- and ViT-backbones on three different datasets, outperforming current state-of-the-art methods.

Acknowledgment

This work was partially supported by JST Moonshot R&D Grant Number JPMJPS2011, CREST Grant Number JPMJCR2015 and Basic Research Grant (Super AI) of In-

stitute for AI and Beyond of the University of Tokyo.

References

- [1] Dian Chen, Dequan Wang, Trevor Darrell, and Sayna Ebrahimi. Contrastive test-time adaptation. In *Proceedings of the IEEE/CVF Conference on Computer Vision and Pattern Recognition*, pages 295–305, 2022. 6
- [2] Haoran Chen, Zuxuan Wu, Xintong Han, and Yu-Gang Jiang. Multi-prompt alignment for multi-source unsupervised domain adaptation. *arXiv preprint arXiv:2209.15210*, 2022. 3
- [3] Zhekai Du, Jingjing Li, Hongzu Su, Lei Zhu, and Ke Lu. Cross-domain gradient discrepancy minimization for unsupervised domain adaptation. In *Proceedings of the IEEE/CVF conference on computer vision and pattern recognition*, pages 3937–3946, 2021. 6
- [4] Alex Fang, Albin Madappally Jose, Amit Jain, Ludwig Schmidt, Alexander Toshev, and Vaishaal Shankar. Data filtering networks. *arXiv preprint arXiv:2309.17425*, 2023. 2
- [5] Yaroslav Ganin, Evgeniya Ustinova, Hana Ajakan, Pascal Germain, Hugo Larochelle, François Laviolette, Mario Marchand, and Victor Lempitsky. Domain-adversarial training of neural networks. *The journal of machine learning research*, 17(1):2096–2030, 2016. 2
- [6] Yunhe Gao, Xingjian Shi, Yi Zhu, Hao Wang, Zhiqiang Tang, Xiong Zhou, Mu Li, and Dimitris N Metaxas. Visual prompt tuning for test-time domain adaptation. *arXiv preprint arXiv:2210.04831*, 2022. 6
- [7] Chunjiang Ge, Rui Huang, Mixue Xie, Zihang Lai, Shiji Song, Shuang Li, and Gao Huang. Domain adaptation via prompt learning. *arXiv preprint arXiv:2202.06687*, 2022. 2, 3, 5, 6
- [8] Geoffrey Hinton, Oriol Vinyals, and Jeff Dean. Distilling the knowledge in a neural network. *arXiv preprint arXiv:1503.02531*, 2015. 3, 4
- [9] Chao Jia, Yinfei Yang, Ye Xia, Yi-Ting Chen, Zarana Parekh, Hieu Pham, Quoc Le, Yun-Hsuan Sung, Zhen Li, and Tom Duerig. Scaling up visual and vision-language representation learning with noisy text supervision. In *International conference on machine learning*, pages 4904–4916. PMLR, 2021. 2
- [10] Guoliang Kang, Lu Jiang, Yi Yang, and Alexander G Hauptmann. Contrastive adaptation network for unsupervised domain adaptation. In *Proceedings of the IEEE/CVF conference on computer vision and pattern recognition*, pages 4893–4902, 2019. 6
- [11] Donghyun Kim, Kaihong Wang, Stan Sclaroff, and Kate Saenko. A broad study of pre-training for domain generalization and adaptation. In *ECCV*, pages 621–638. Springer, 2022. 2, 3
- [12] Zhengfeng Lai and et al. Padclip: Pseudo-labeling with adaptive debiasing in clip for unsupervised domain adaptation. In *Proceedings of the IEEE/CVF International Conference on Computer Vision*, pages 16155–16165, 2023. 3, 5, 6
- [13] Zhengfeng Lai and et al. Empowering unsupervised domain adaptation with large-scale pre-trained vision-language models. In *Proceedings of the IEEE/CVF Winter Conference on Applications of Computer Vision*, pages 2691–2701, 2024. 3, 5, 6
- [14] Junjie Li, Yixin Zhang, Zilei Wang, and Keyu Tu. Probabilistic contrastive learning for domain adaptation. *arXiv preprint arXiv:2111.06021*, 2021. 5
- [15] Jian Liang, Dapeng Hu, and Jiashi Feng. Do we really need to access the source data? source hypothesis transfer for unsupervised domain adaptation. In *International Conference on Machine Learning*, pages 6028–6039. PMLR, 2020. 2, 6
- [16] Mingsheng Long, Zhangjie Cao, Jianmin Wang, and Michael I. Jordan. Conditional adversarial domain adaptation. In *NeurIPS*, pages 1647–1657, 2018. 2, 3, 5, 6, 7
- [17] Zhihe Lu, Yongxin Yang, Xiatian Zhu, Cong Liu, Yi-Zhe Song, and Tao Xiang. Stochastic classifiers for unsupervised domain adaptation. In *Proceedings of the IEEE/CVF Conference on Computer Vision and Pattern Recognition*, pages 9111–9120, 2020. 6
- [18] Jaemin Na, Dongyoon Han, Hyung Jin Chang, and Wonjun Hwang. Contrastive vicinal space for unsupervised domain adaptation. In *European Conference on Computer Vision*, pages 92–110. Springer, 2022. 6
- [19] Xingchao Peng, Qinxun Bai, Xide Xia, Zijun Huang, Kate Saenko, and Bo Wang. Moment matching for multi-source domain adaptation. In *ICCV*, pages 1406–1415, 2019. 7
- [20] Xingchao Peng, Ben Usman, Neela Kaushik, Judy Hoffman, Dequan Wang, and Kate Saenko. Visda: The visual domain adaptation challenge. *arXiv preprint arXiv:1710.06924*, 2017. 7
- [21] Hieu Pham, Zihang Dai, Golnaz Ghiasi, Kenji Kawaguchi, Hanxiao Liu, Adams Wei Yu, Jiahui Yu, Yi-Ting Chen, Minh-Thang Luong, Yonghui Wu, et al. Combined scaling for zero-shot transfer learning. *Neurocomputing*, 555:126658, 2023. 2
- [22] Viraj Prabhu, Shivam Khare, Deeksha Kartik, and Judy Hoffman. Sentry: Selective entropy optimization via committee consistency for unsupervised domain adaptation. In *Proceedings of the IEEE/CVF International Conference on Computer Vision*, pages 8558–8567, 2021. 2, 5
- [23] Alec Radford, Jong Wook Kim, Chris Hallacy, Aditya Ramesh, Gabriel Goh, Sandhini Agarwal, Girish Sastry, Amanda Askell, Pamela Mishkin, Jack Clark, et al. Learning transferable visual models from natural language supervision. In *International conference on machine learning*, pages 8748–8763. PMLR, 2021. 2, 5, 6
- [24] Harsh Rangwani, Sumukh K Aithal, Mayank Mishra, Arihant Jain, and Venkatesh Babu Radhakrishnan. A closer look at smoothness in domain adversarial training. In *International Conference on Machine Learning*, pages 18378–18399. PMLR, 2022. 5
- [25] Mainak Singha, Harsh Pal, Ankit Jha, and Biplab Banerjee. Ad-clip: Adapting domains in prompt space using clip. In *Proceedings of the IEEE/CVF International Conference on Computer Vision*, pages 4355–4364, 2023. 3, 5, 6
- [26] Tao Sun, Cheng Lu, Tianshuo Zhang, and Haibin Ling. Safe self-refinement for transformer-based domain adaptation. In

- Proceedings of the IEEE/CVF conference on computer vision and pattern recognition*, pages 7191–7200, 2022. 5, 6
- [27] Hui Tang, Ke Chen, and Kui Jia. Unsupervised domain adaptation via structurally regularized deep clustering. In *Proceedings of the IEEE/CVF conference on computer vision and pattern recognition*, pages 8725–8735, 2020. 5
- [28] Hemant Venkateswara, Jose Eusebio, Shayok Chakraborty, and Sethuraman Panchanathan. Deep hashing network for unsupervised domain adaptation. In *CVPR*, pages 5018–5027, 2017. 7
- [29] Thomas Westfechtel, Hao-Wei Yeh, Qier Meng, Yusuke Mukuta, and Tatsuya Harada. Backprop induced feature weighting for adversarial domain adaptation with iterative label distribution alignment. In *Proceedings of the IEEE/CVF Winter Conference on Applications of Computer Vision*, pages 392–401, 2023. 5
- [30] Thomas Westfechtel, Hao-Wei Yeh, Dexuan Zhang, and Tatsuya Harada. Gradual source domain expansion for unsupervised domain adaptation. In *Proceedings of the IEEE/CVF Winter Conference on Applications of Computer Vision*, pages 1946–1955, 2024. 3, 5
- [31] Shaoan Xie, Zibin Zheng, Liang Chen, and Chuan Chen. Learning semantic representations for unsupervised domain adaptation. In *International conference on machine learning*, pages 5423–5432. PMLR, 2018. 2
- [32] Tongkun Xu, Weihua Chen, Pichao Wang, Fan Wang, Hao Li, and Rong Jin. Cdtrans: Cross-domain transformer for unsupervised domain adaptation. *arXiv preprint arXiv:2109.06165*, 2021. 2, 5
- [33] Jinyu Yang, Jingjing Liu, Ning Xu, and Junzhou Huang. Tvt: Transferable vision transformer for unsupervised domain adaptation. In *Proceedings of the IEEE/CVF Winter Conference on Applications of Computer Vision*, pages 520–530, 2023. 2, 5
- [34] Giacomo Zara, Alessandro Conti, Subhankar Roy, Stéphane Lathuilière, Paolo Rota, and Elisa Ricci. The unreasonable effectiveness of large language-vision models for source-free video domain adaptation. In *Proceedings of the IEEE/CVF International Conference on Computer Vision*, pages 10307–10317, 2023. 3
- [35] Xiaohua Zhai, Xiao Wang, Basil Mustafa, Andreas Steiner, Daniel Keysers, Alexander Kolesnikov, and Lucas Beyer. Lit: Zero-shot transfer with locked-image text tuning. In *Proceedings of the IEEE/CVF Conference on Computer Vision and Pattern Recognition*, pages 18123–18133, 2022. 2
- [36] Sicheng Zhao, Xiangyu Yue, Shanghang Zhang, Bo Li, Han Zhao, Bichen Wu, Ravi Krishna, Joseph E Gonzalez, Alberto L Sangiovanni-Vincentelli, Sanjit A Seshia, et al. A review of single-source deep unsupervised visual domain adaptation. *IEEE Transactions on Neural Networks and Learning Systems*, 33(2):473–493, 2020. 2
- [37] Kaiyang Zhou, Jingkang Yang, Chen Change Loy, and Ziwei Liu. Learning to prompt for vision-language models. *International Journal of Computer Vision*, 130(9):2337–2348, 2022. 3
- [38] Jinjing Zhu, Haotian Bai, and Lin Wang. Patch-mix transformer for unsupervised domain adaptation: A game perspective. In *Proceedings of the IEEE/CVF Conference on Computer Vision and Pattern Recognition*, pages 3561–3571, 2023. 2, 5, 6
- [39] Fuzhen Zhuang, Zhiyuan Qi, Keyu Duan, Dongbo Xi, Yongchun Zhu, Hengshu Zhu, Hui Xiong, and Qing He. A comprehensive survey on transfer learning. *Proceedings of the IEEE*, 109(1):43–76, 2020. 2